Up to this point we have focused on the computation of formation dips from resistivity and acoustic images. Initially the primary use for the dipmeter tools focused on structural dip computation from one borehole rather than three boreholes .Dips are also used to define Sedimentologic features and this application became reality upon the advent of correlation techniques using computers in the early 1960’s.

The advent of resistivity imaging tools in the late 1970’s early 1980’s produced data that provided a much more detailed picture of the borehole wall. Integration with cores and direct comparison became a realistic approach. The amount of information acquired in the borehole for dip and Imagelog Interpretation today allows the following categories of interpretation to be done.

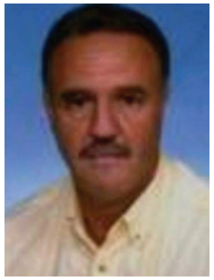

Rafik Baouche received a Magister degree in Geophysical Applications from the University of Boumerdes (Algeria) and a Doctorate of Earth Sciences from the University of Boumerdes and University of Rennes1, France in 2008. He is currently a member of the Laboratory of the Earth Sciences in the Faculty of Hydrocarbons and Chemistry at Boumerdes(3500)

978-620-2-68193-3

Rafik Baouche

Image log Processing and Interpretation

Interpretation of well imaging by electrical logging

LAP LAMBERT Academic Publishing

Rafik Baouche

Image log Processing and Interpretation

Rafik Baouche

Image log Processing and Interpretation

Interpretation of well imaging by electrical logging

LAP LAMBERT Academic Publishing

Imprint
Any brand names and product names mentioned in this book are subject to trademark, brand or patent protection and are trademarks or registered trademarks of their respective holders. The use of brand names, product names, common names, trade names, product descriptions etc. even without a particular marking in this work is in no way to be construed to mean that such names may be regarded as unrestricted in respect of trademark and brand protection legislation and could thus be used by anyone.

Cover image: www.ingimage.com

Publisher:
LAP LAMBERT Academic Publishing
is a trademark of
International Book Market Service Ltd., member of OmniScriptum Publishing Group
17 Meldrum Street, Beau Bassin 71504, Mauritius
Printed at: see last page
ISBN: 978-620-2-68193-3

Manual for use by geologists, geophysicists and producers

Interpretation of well imaging by electrical logging

Par Mr BAOUCHE RAFIK
(Maître de Conférence – Dpt de géophysique

Summary

Imagelog Interpretation Overview

Up to this point we have focused on the computation of formation dips from resistivity and acoustic images. Initially the primary use for the dipmeter tools focused on structural dip computation from one borehole rather than three boreholes .Dips are also used to define Sedimentologic features and this application became reality upon the advent of correlation techniques using computers in the early 1960's.
The advent of resistivity imaging tools in the late 1970's early 1980's produced data that provided a much more detailed picture of the borehole wall. Integration with cores and direct comparison became a realistic approach. The amount of information acquired in the borehole for dip and Imagelog Interpretation today allows the following categories of interpretation to be done:

- Structural Dip Interpretation: determine the following information from Structural Dip Analysis:
  - Dip Magnitude
  - Structural Type
  - Fracture orientation and type
  - Fault/Fracture Plunge
  - Stress Regime orientation
  - Sedimentologic Dip Interpretation: remove the structural dip to help determine the following information:
  - Sand Body Morphology
  - Paleocurrent inference
  - Depositional Environment
  - Thin Bed porosity/permeability characterisation
  - Clastic Environments: Imagelog Interpretation features in Clastic Environments
  - Carbonate Environments: Imagelog Interpretation features in Carbonate Environments
  - Thin Bed Analysis: High Resolution determination of petrophysical properties in conjunction with standard resolution logs
  - Reservoir Heterogeneity: Carbonate Rock Fabric properties
  - Borehole Mechanics: Sanding Analysis, Borehole breakout and stability

In order to usefully apply image data to the above problems, the interpretation involves use of techniques which involve auxiliary plots that can be generated from the dip data either manually picked or automatically generated. If manually picked data is used, the features picked can be distinguished based on lithology, dip magnitude, feature character and observed dip trends. When utilizing Petrolog we can generate the following useful graphics objects:

- Stereonets: Wulff, Schmidt and Walkout plots
- Stick Plots:
- Azimuth Rose:
- Breakout Plots
- Breakout Perspective
- Breakout Rose

These plots are designed to present spatial information in 2 dimensions and in a format that allows relationships to be readily determined and related to the geologic environment.

Imagelog Interpretation: Structural Dip Interpretation

Structural dip is defined as a regional dip trend which describes the attitude of a particular formation in the crust. It is generally represented by the dip in shales and is usually inferred from intervals of consistent dip that are of such a length that reasonably defines the regional trend. Before any Paleocurrent work can be undertaken, structural dip needs to be determined and removed. An example of structural dip is illustrated in the following figure 1

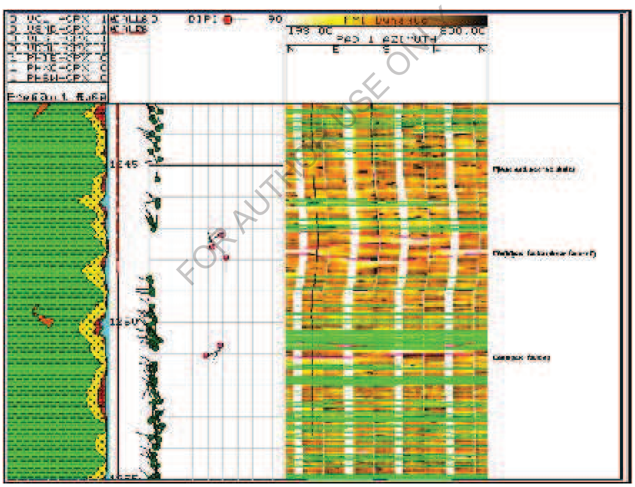

Figure 1

These structural dips can be plotted as stick plots and when plotted in time can give a realistic comparison with seismic. This has application in assessing accuracy of time to depth conversion. Velocity field estimation etc. An example of the comparison is illustrated in figure 2

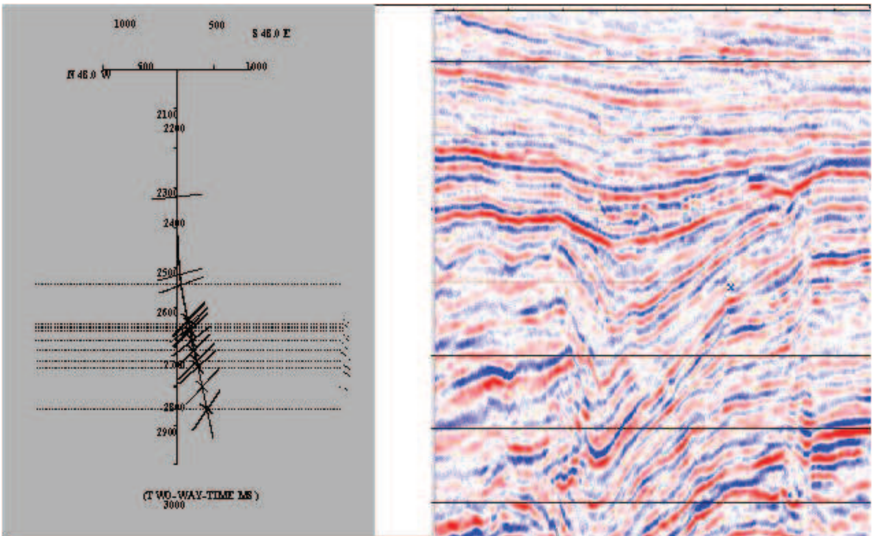

Figure 2

Figure 2 shows a stick plot presentation next to a seismic plot.

Faulting within an interval can be identified on an image as a discordant break or change in formation type. On single button dip resistivity data, the presence of a fault was inferred from deformation envelopes surrounding the actual fault or fault zone. A deformation envelope is local ductile deformation associated with the fault or fault drag. The fault drag usually presents itself as increasing then decreasing dip magnitude as illustrated in figure 3.

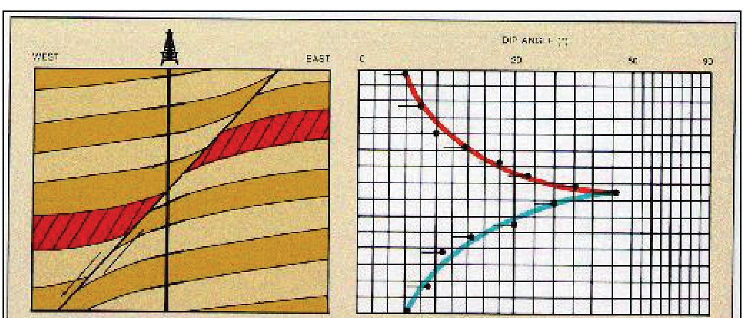

Fig. 5-19 — Drag often produces small concave folds in downthrown block and small convex folds in the upthrown block.

Figure 3

Figure 3 is a typical fault drag and the resultant dip pattern on the right. See Fundamentals of Dip Log Analysis Atlas Wireline Services Western Atlas (Bigelow, 1987)

If the pole to the plane of these dips is plotted on an equal area lower hemisphere stereonet they will describe a great circle. The pole to the plane of the great circle describes the plunge of the fold or the orientation of the fold.

The drag may be produced on either the foot wall or the hanging wall or both.

The amount of detail present in the images available today permits identification of faults that are down to the centimeter scale. The examples in figure 4 show faults that do not have a deformation envelope but have juxtaposed discordant bedding:

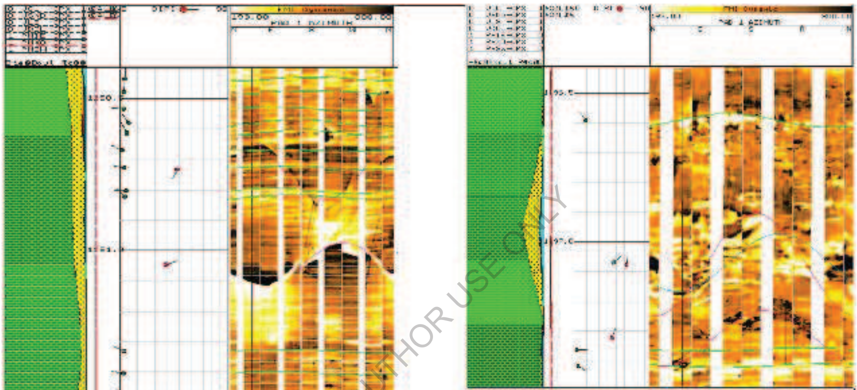

Figure 4

Figure 4 are Images showing small scale faulting (both images cover a 2 Meter Interval)

Fractures identification is also an important part of structural analysis and can define important structural trends related to porosity and the structural style of the field. By identifying fracture frequency and the average dip, the true spacing can be determined. The distribution of fractures can have a marked affect on the productibility and the ultimate recovery of a reservoir. The orientation of fractures in space can assist in describing the structural style of a particular reservoir. The example illustrated in Figure 5 shows fractures (blue and green picks) occurring at or near what could be considered to be a fault zone. A distinct conjugate set is defined by these fractures with a Northwest and Southeast dip direction orientation.

These fractures can be used to define the true fracture spacing not the fracture spacing as illustrated on the plot. The methodology for doing this is illustrated in figure 6.

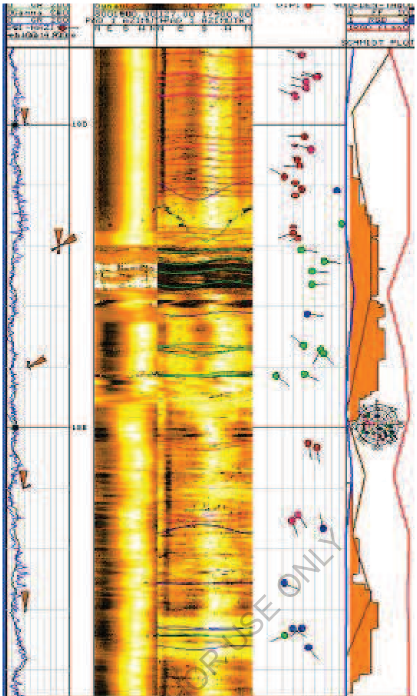

Figure 5

Figure 5 shows fractures illustrating a conjugate set.

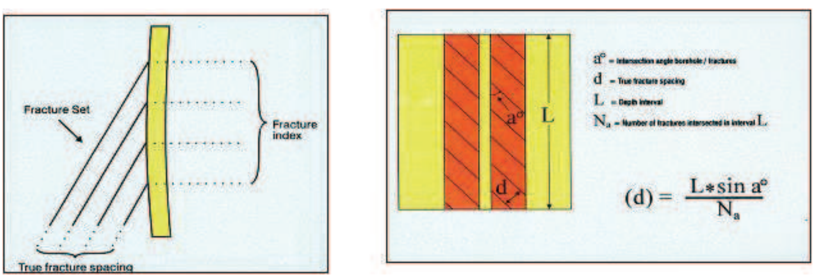

Figure 6

Figure 6 gives the equation used in the determination of true fracture spacing

The deformation associated with faults and also with folds can be used to define the fold. By plotting the dips on a equal area lower hemisphere stereonet as poles to plane of the dips permits the use of the spherical geometric properties of the stereonet to identify fold axis and plunge. These fold geometries are illustrated in figure 7.

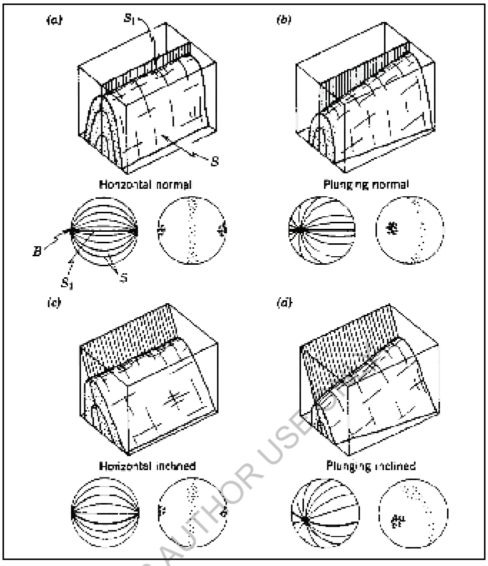

Figure 7

Figure 7 illustrates fold identification from an unknown reference.

Geometrically, a fold should have a dip arrangement that creates great circles that intersect at the plunge. Because this is confusing, the approach usually taken is to plot the poles and see if the dips create a shape that represents a great circle. Various examples are shown in the above stereonets.

Bengston (1981) introduced a statistical technique that is now abbreviated SCAT. It essentially takes the dips and constructs transverse and longitudinal sections oriented along structure and down dip from structure. The transverse section is oriented in the dip direction where the greatest cluster of dip magnitude exists. His figures on the next pages illustrate how the dips are presented.

Rather than just computing the apparent dip, the technique relies on computation of the variance of the dip from the longitudinal and transverse directions. The fold or fault type can be distinguished through different patterns. These patterns also permit the definition of anticline, syncline and throw orientation on the fault.

A great circle is constructed on a stereonet as follows. Rotate the stereonet so that the strike (dip direction -90 Deg) of the dip is at 0 degrees or North point. The dip magnitude is counted in from the edge on the right hand (East) side of the Stereonet. The pole is plotted as a point 90 degrees away. That is you count out from the centre on the west side of the plot the dip magnitude whilst keeping the net in this orientation.

Ref Bengston., Statistical Curvature Analysis Techniques for Structural Interpretation of Dipmeter Data, AAPG Bulletin, V. 65, 1981,PP 312-332

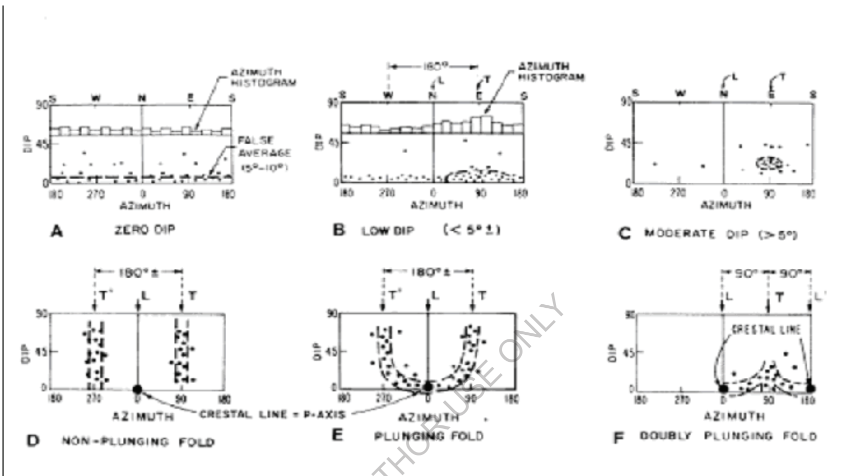

FIG. 2—Six basic dip versus azimuth patterns corresponding to bulk-curvature categories of Figure 1.

Figure 8

Figure 8 shows the different scatter patterns for different tectonic settings.

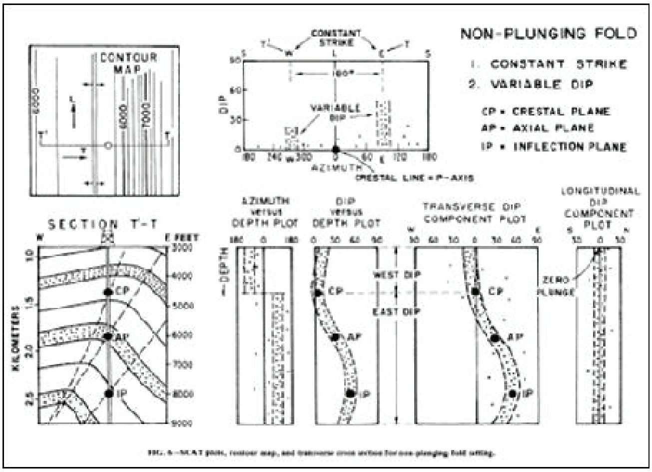

Figure 9

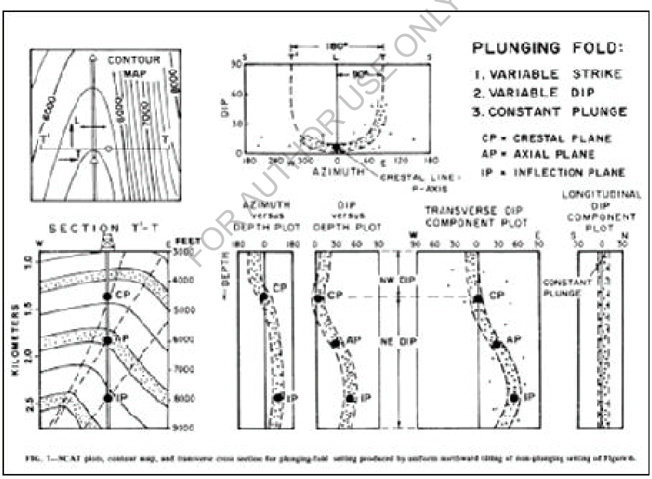

Figure 10

Figure 9 and 10: Bengston (1981) Scatter patterns for different tectonic settings.

Imagelog Interpretation: Sedimentologic Dip Interpretation

Earlier we showed that dipmeter and later images were used to fulfill a need to identify structural dip of formations so that future wells could be better planned. The initial development of the dipmeter coincided at a time when surface mapping and basic low fold seismic were used to locate wells. Early workers such as Gilreath ,(1960) Gilreath and Maricelli (1964) and Campbell (1968) recognized the value of these tools in determining sedimentary dips. The advent of computer processed dips greatly enhanced the ability to use this data.

The original techniques involved recognition of patterns in the dip data and attributing tectonic or depositional significance to the dips. Gilreath and Maricelli, (1964) summarizes the dip patterns in figure 1.

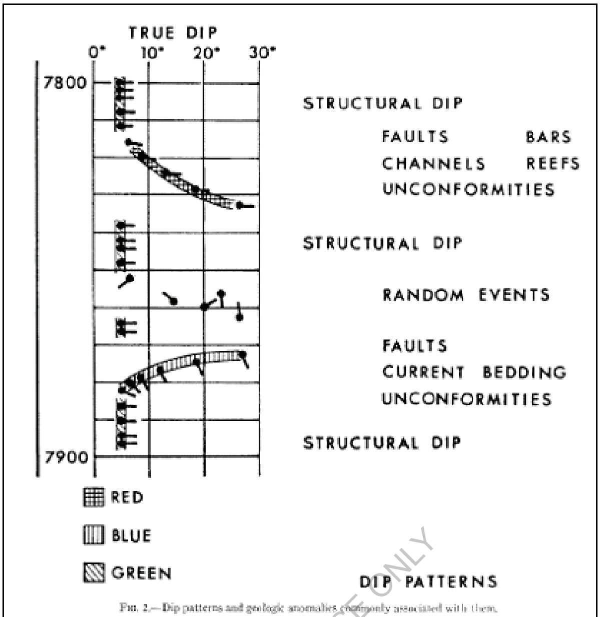

Figure 1

Figure 1: Detailed Stratigraphic Control Through Dip Computations AAPG Bulletin Vol. 48 No 12 (Gilreath and Maricelli, 1964)

These patterns represented trends seen as follows: Green patterns were used to indicate structural dip. Structural dip was generally considered to be represented in shales or quiescent sediments and have significant intervals of consistent dip. Comparing this with image data in Figure 4 shows structural dip.

Patterns that showed consistent trends such as increasing dip magnitudes with depth and decreasing dip magnitude with depth were observed to coincide with particular geological formations or units. In order to interpret the dip patterns a basic understanding of the depositional environment is required. Note that from the above figure, the red pattern could be interpreted in the context of fault deformation, bars, channels or reefs. This pattern in a fluvial sand is illustrated in Figure 3

Patterns associated with decreasing dip magnitude with depth are associated with faults, current bedding or unconformities. These patterns are illustrated in Figure 4. Again the context for interpretation is determined by the geological setting in which the pattern is found.

Jizba et al (1964) compared dip profiles with core. They compared 2000 ft of nearly continuous core with a 3 arm dipmeter survey and observed that the resistivity profiles were similar. However, whilst the resistivity inflexions and subsequently dip computations broadly matched the core, certain features could not be explained by lithological variations. The examples cited were a result of variations in cementation. One question they raised was that, given the success through the use of both manual and computer generated dip computations together with subsequent interpretation, the interpretation based on application of the above methodology needs to be fully understood.

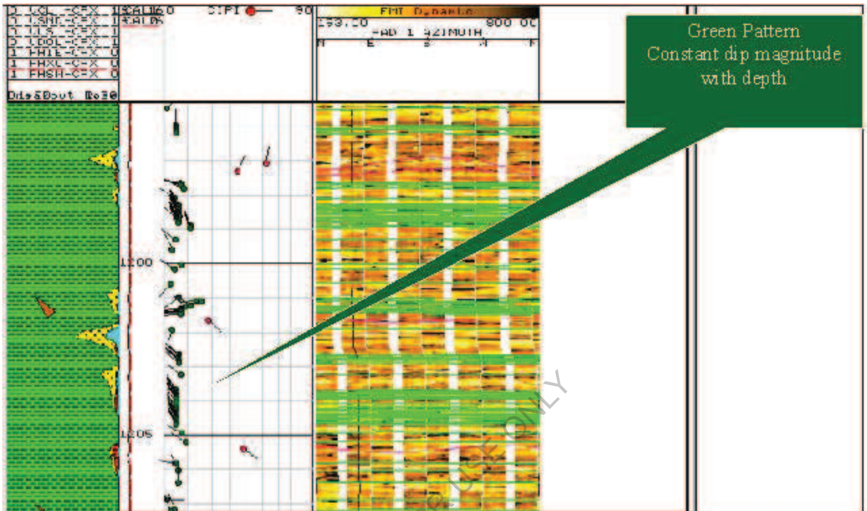

Figure 2

Figure 2 Structural Dip illustrated. This example shows a 3 degree NW

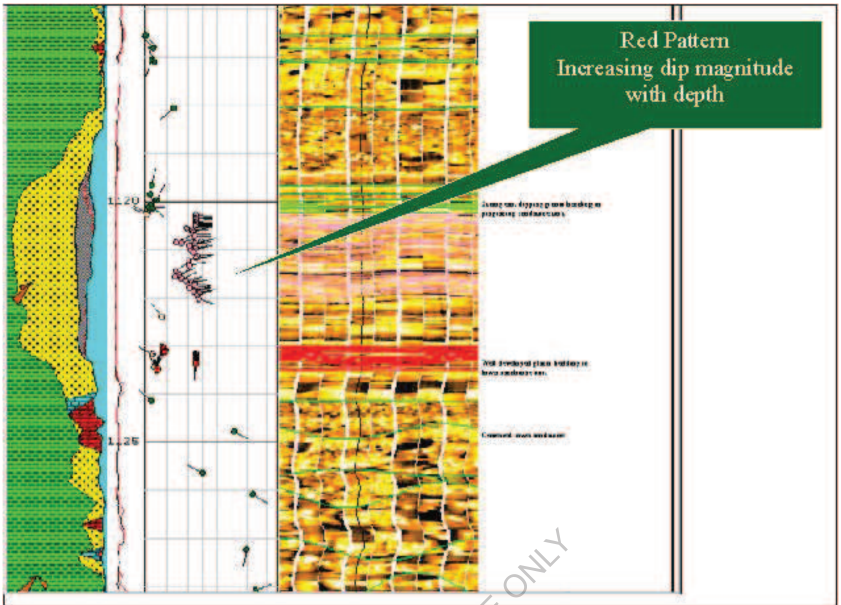

Figure 3

Figure 3: The red dips show red pattern showing an East structural dip

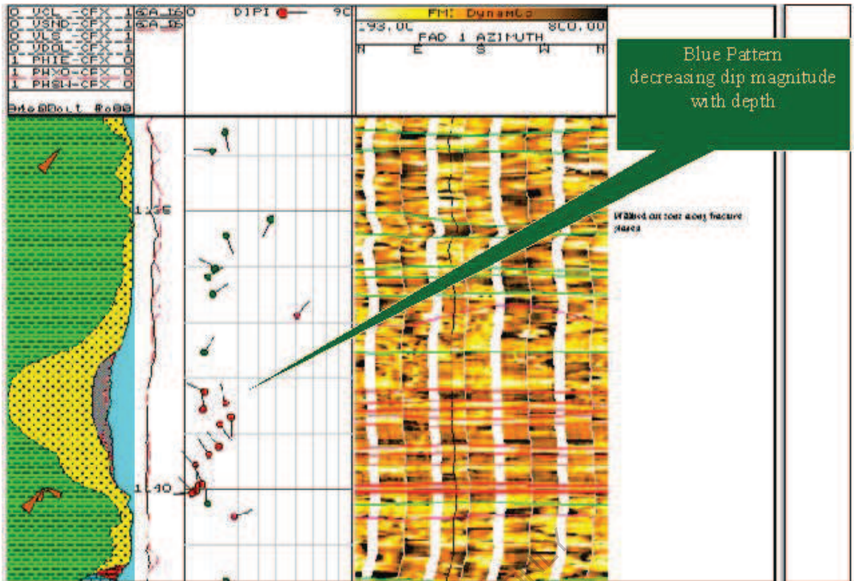

Figure 4

Figure 4 Structural Dip illustrated. This example shows a 3 degree NW

With the advent of imaging tools, vastly greater amounts of information can be extracted from the images beyond paleo current information as derived from the dip data and pattern interpretation. However, before discussing these, let's compare the original scheme illustrated by Campbell (1968) with bedding system setup by Miall (1996). The scheme developed by Miall is based on bedding and showed that set boundaries and coset boundaries that had a dip separation to intraset surfaces of 60 degrees or greater are laterally accreting. Combining this with an understanding of what depositional environment may be most likely, has allowed the development of classification schemes that are consistent and relate to paleo current more directly.

A comparison of Miall's basic classification with the initial scheme (Campbell 1968) in Figure 167 shows that the understanding of lateral accretion versus pro-gradation was implicit in the initial development of the pattern interpretation scheme. The problem with the pattern interpretation scheme is that it is too simplistic and does not accommodate the additional information that can be identified in an image.

When classifying dips to be more meaningful than just purveying bed attitude the scheme used has to be consistent and not controversial. Picks classified need to be easily identified as such with any other users of the data. To this end, combining a systematic bed definition approach such as suggested in Miall (1996) in classifying dips from image will fulfill these criteria. A suitable classification scheme may be illustrated as follows:

Name	General Use	Description	Typical Log responses
Shale	Structural Dip and quiescent sediment	Shales identified by observing log responses that can be used to identify structural and other tectonic features.	GR high, Resistivity low, Neutron-density indicative of high porosity and erratic. Caliper indicative of washout
Fractures	Fractures, Faults discordant features in the image	Fractures and faults can be described as resistive or conductive. This often depends on cement or fill type which can be resistive or conductive	Features usually are not of such an areal extent that they create a response effect. The caliper may indicate a sharp increase in size with some fractures.
Planar bedding	Sand or silt bedding that l parallel	Sand or silt bedding can be parallel may indicate laminar flow (high energy deposition)	Low Gamma Ray Neutron-Density gives general sand response Resistivity responds to Rw in formation Caliper usually in gauge
Cross bedding	Sand or Silt	Sand or silt may have bedding features that are discontinuous. Show typical micro red and micro blue patterns indicating short cycles of accretion or progradation	Low Gamma Ray Neutron-Density gives general sand response Resistivity responds to Rw in formation Caliper usually in gauge

Figure 5

Name	General Use	Description	Typical Log responses
Intraset Bedding	Similar to planar bedding but usually inclined. Discordant at set boundary bedding surfaces that indicate erosion or deposition of new bedding set. Usually consistently in one direction within sets	Sand or silt. Again bedding consistent and clean.	Low Gamma Ray Neutron-Density gives general sand response Resistivity responds to Rw in formation Caliper usually in gauge
Set boundaries	Surface that defines the change from two intraset bedding groups that are dipping	When mapping bedding, the intraset surfaces usually define lateral accretion or progradation of a particular bedding. When a new bedding group commences, it has the same dip direction as the previously deposited intraset.	Low Gamma Ray Neutron-Density gives general sand response Resistivity responds to Rw in formation Caliper usually in gauge
Coset boundaries	Surface that defines a boundary between two intra set groups that have different dip orientations	Intraset surface orientations may vary indicating different sources. The source could simply reflect a change in channel direction.	Low Gamma Ray Neutron-Density gives general sand response Resistivity responds to Rw in formation Caliper usually in gauge
Heterolithics	Surfaces that occur in thin bedded sediment	These surfaces may be representative of a crevasse-splay, tidal channel, near shore or other deposits where sand and clay get deposited in equal quantities.	Medium Gamma Ray Neutron density indicative of shale or sand depending on ratio Resistivity may have depressed response if hydrocarbon bearing.
Vugs	Carbonate vugs	Generally holes in carbonate	Limestone or dolomite response.

Figure 6

Figure 5,6: Miall, A., The Geology of Fluvial Deposits: Sedimentary Facies, Basin Analysis, and Petroleum Geology, Springer Verlag; (January 1996)

Generally the picks for carbonates should be similar to clastics however; there will be less in the way of bedding as carbonates will have more biogenic features.

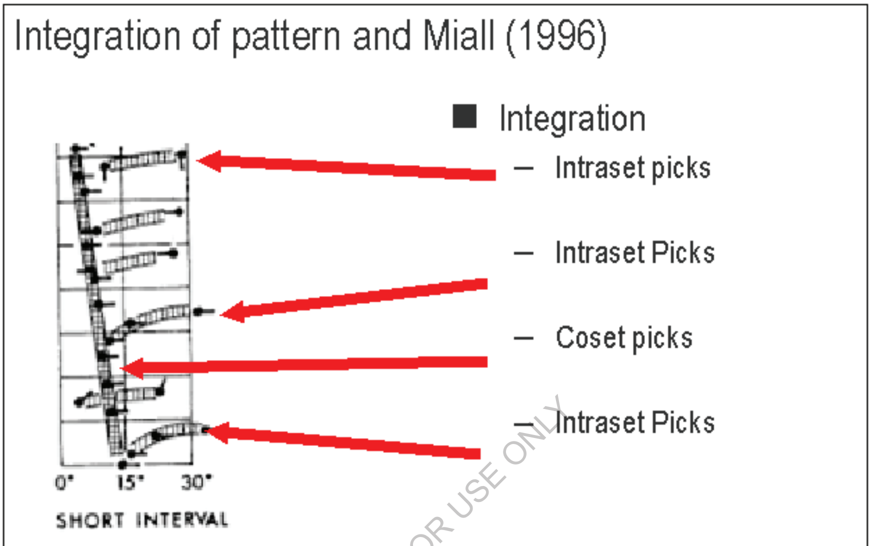

Figure 7

Figure 7 Comparison of Campbell (1964) with Miall (1996)

When applying these classifications, consistencies are keys to good and reproducible interpretation. The following figure shows the zoning of the interval showing the classification prior to actual picking.

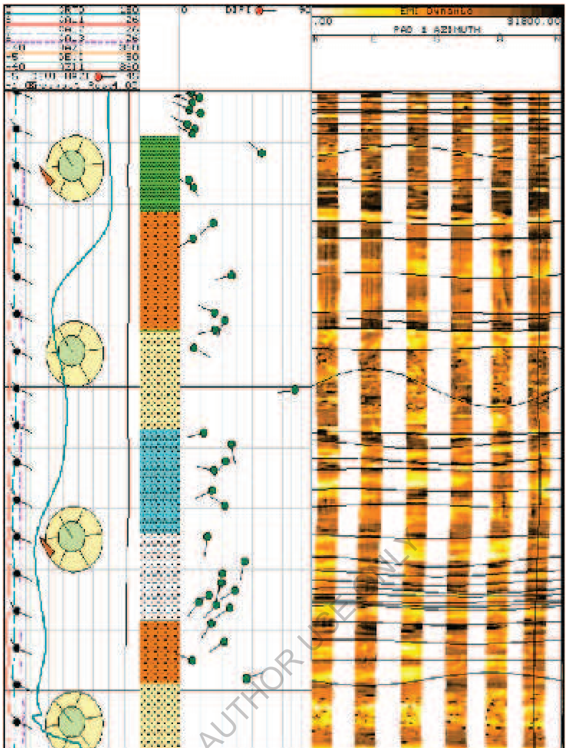

Figure 8

Figure Coloured column shows zonations as per bedding. Note the yellow zones have clasts and little bedding.

When classified the dip patterns look as in figure 9.

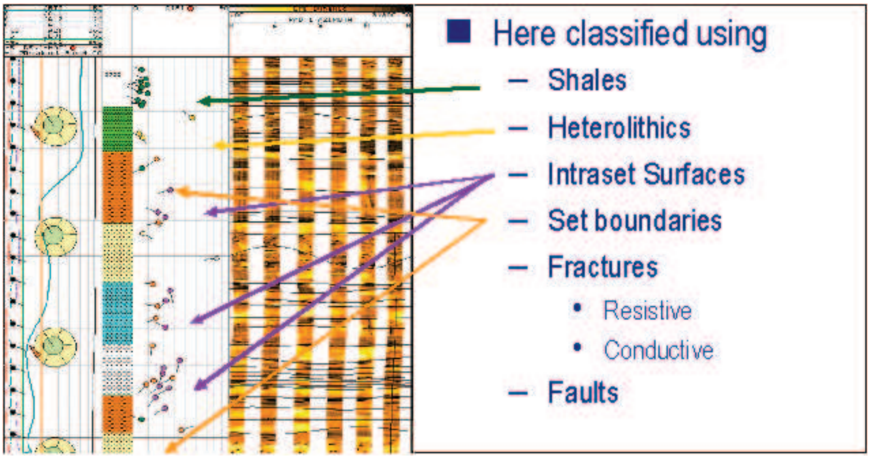

Figure 9

Figure 9 Coloured column shows zonation as per bedding. Note the yellow zones have clasts and little bedding.)

Auxiliary plots become important when analyzing the data. The walkout plot as illustrated in the next diagram shows that the interval examined has a depositional trend to the ENE. There is predominantly pro-gradation in the interval but lateral accretion is visible at a couple of points. Structural dip must be removed prior to any paleocurrent analysis.

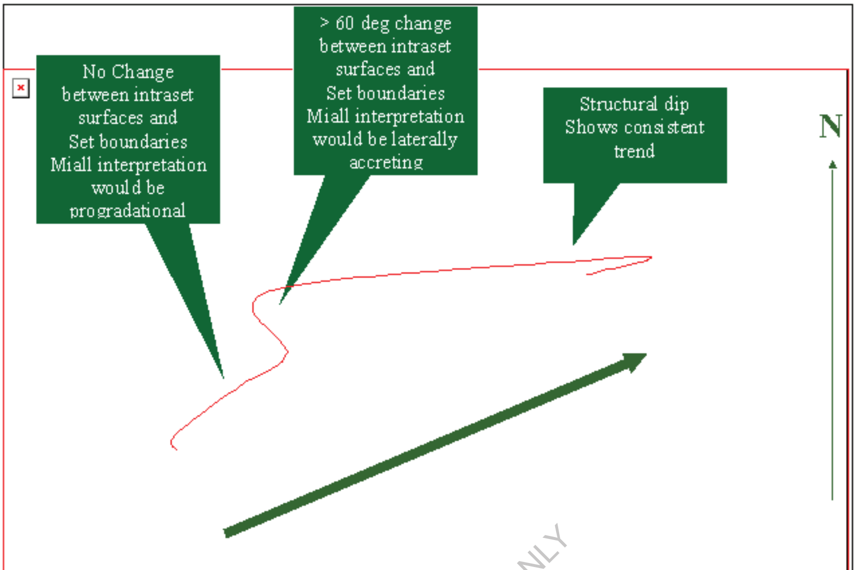

Figure 10

Figure 10 Walkout Plot showing dip trend from previous Figure

The paleocurrent analysis will generally fall into four categories:

1. Unimodal mode – Perpendicular to current
2. Bipolar azimuthal patterns in cross bedding deposited by unidirectional currents
3. Bipolar cross bedding with transport axis perpendicular to angle of repose e.g.: seif dunes
4. Bipolar paleocurrents with perpendicular mode e.g.: turbidite erosional and slump structures

Schmidt, Wolf and Rose plots also aid in the identification of paleocurrent analysis.

In addition to the identification of paleocurrent analysis, a fabric or bioturbation index can be created using the fracture frequency function. This index can be used as an indicator of bioturbation or energy level. Taking the example we are working through here, the energy levels can be illustrated as follows:

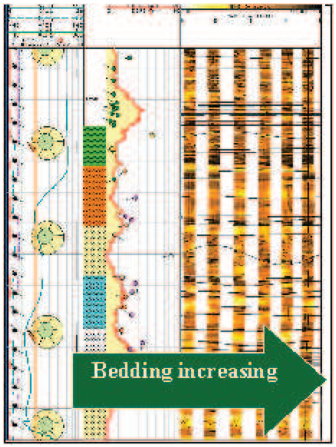

Figure 11

Figure 11 Bioturbation/Fabric Index – note the yellow zones are low and the red zones moderate

By combining the paleocurrent with the bioturbation/fabric index and lithology, other interpretive remarks from the image, a good deal of information about the formation can be identified and presented.

Imagelog Interpretation: Clastic Environments

The previous section put forward some guidelines for the interpretation of dip data. The most important factor in interpretation is understanding typically what depositional environment is expected and what paleocurrent and image character can reasonably be expected. There are similarities in a number of environments that make interpretation ambiguous. In these cases the application of ichno-fabric, bio-stratigraphy, log response character and direct core interpretation become critical to the correct interpretation.

Fluvial Environments

The application of dip or image interpretation is dependent on the depositional environment encountered. Each environment will present challenges that are different however, by applying the consistent approach discussed previously good interpretations about architecture can be achieved. An unknown author has compiled a number of figures showing various depositional models. These are illustrated here below.

These figures illustrate models for the various fluvial depositional environments. Included on them is a log profile with typical rose plots presented. This section briefly covers some main clastic environments and the types of paleocurrent patterns and associated log responses. The figures cover braided channel, point bar, lacustrine delta fill, bay fill, abandoned distributary channel, mouth bar, tidal ridges and subaqueous slumps. In summarizing each figure, significant ambiguity will become apparent. Other information is required to place the interpretation in the right context.

Braided channels have generally upward fining profiles. The sequence shows generally pro-gradation dip patterns which can be illustrated in rose plots and walkout plots. When looking at images, identifying root burrowing at the top of each sand interval may help identify the interval. The log motifs that show different positions on a braided stream system illustrate the variability across a stream.

Meandering point bars are the typical deposit that was used to typify the initial red blue pattern interpretation scheme. The log motifs show generally upward fining trends. The main channel is characterized by constant grain size (reflected in uniform low GR values). The Patterns show a wide range of dip orientations however, as pointed out earlier in Sedimentologic Dip Interpretation Techniques, when the azimuthal angle between intraset bedding and set/coset bedding is less than 60 degrees the unit is generally pro-gradational. Translating to architecture, the arrangement permits inferences to be made about reservoir continuity. Laterally accreting systems permit direction to channel centre to be identified whereas pro-grading patterns do not permit this.

Lacustrine fill are characterized by upward coarsening motifs. The rose plots and walkout plots should show pro-gradation in the lake direction. Again, similarity or rather ambiguity means that other information needs to be integrated into the interpretation to permit inference of lacustrine deposit.

Bay Fill deposits are extremely similar to Lacustrine deposits. Log motifs are similar and dip patterns are similar.

Abandoned Distributary channels have inter bedded sand and shales which may or may not be thin bedded. Dip patterns generally give a pro-grading trend.

Distributary mouth bars are upward coarsening and have a pro-grading trend. This trend is very similar to Lacustrine mouth bars and Braided stream facies. Again other information gleaned from core, bio stratigraphy and regional context is necessary to infer this environment.

Tidal Mouth Ridges have the characteristic bi directional paleo-current direction. This is usually well illustrated with rose plots.

Subaqueous slumps are deposits that have syn-depositional movement below the water line. Water escape and liquefaction structures may occur obliterating the dip patterns present. Generally the dip patterns will show a depositional direction that is similar to the slumping direction.

Turbidites

Turbidites are deposits that occur in a deep water environment. Generally they are associated with clastics however; chalk turbidites have been documented in the North Sea. The original work was documented by Bouma who documented basic divisions which were summarized as facies A through E (Figure 158). A comprehensive grain size based review paper was produced by Reading et al . (1994) "Reading et. al., Turbidite Systems in Deep-Water Basin Margins Classified by Grain Size and Feeder System, AAPG Bulletin, V. 78, No. 5 (May 1994), P. 792–822." that documents turbidites on the basis of grain size. They described systems as wedges, channels, lobes and sheets.

The geometry and character of the various turbidites were controlled by the source material (i.e. grain size).

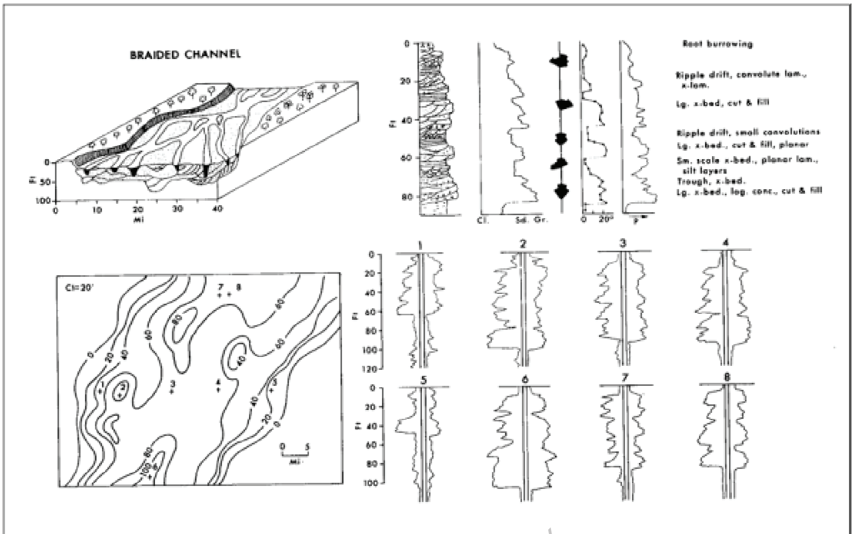

Fig. 3—Summary diagrams illustrating the major characteristics of braided channel deposits (letters on the vertical section refer to core or outcrop photographs).

Figure 1

Figure 1 Braided Channel Stylised Example (Source Unknown)

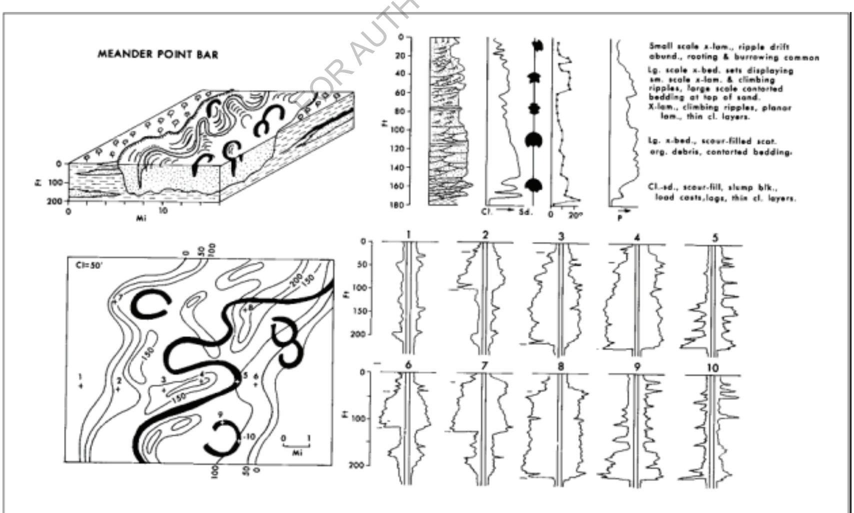

Fig. 4—Summary diagram illustrating the major characteristics of meandering point-bar deposits.

Figure 2

Figure 2 Meander Point Bar Stylised Example (Source Unknown)

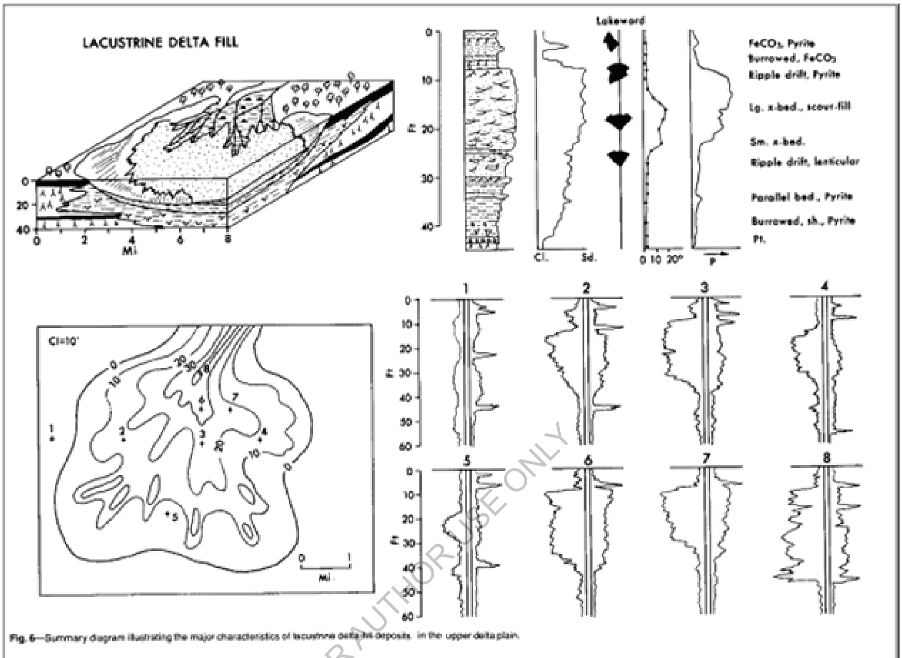

Figure 3

Figure 3 Lacustrine Delta Fill Stylised Example (Source Unknown)

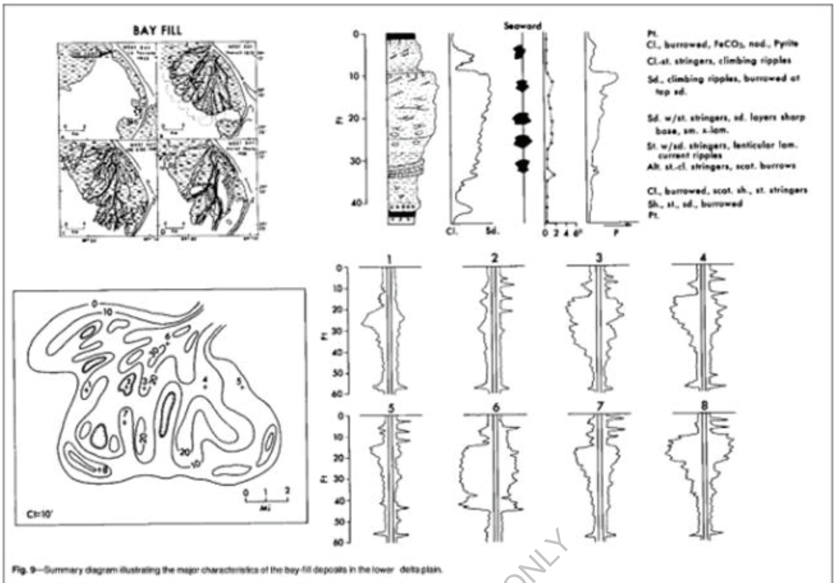

Figure 4

Figure 4 Bay Fill Stylised Example (Source Unknown)

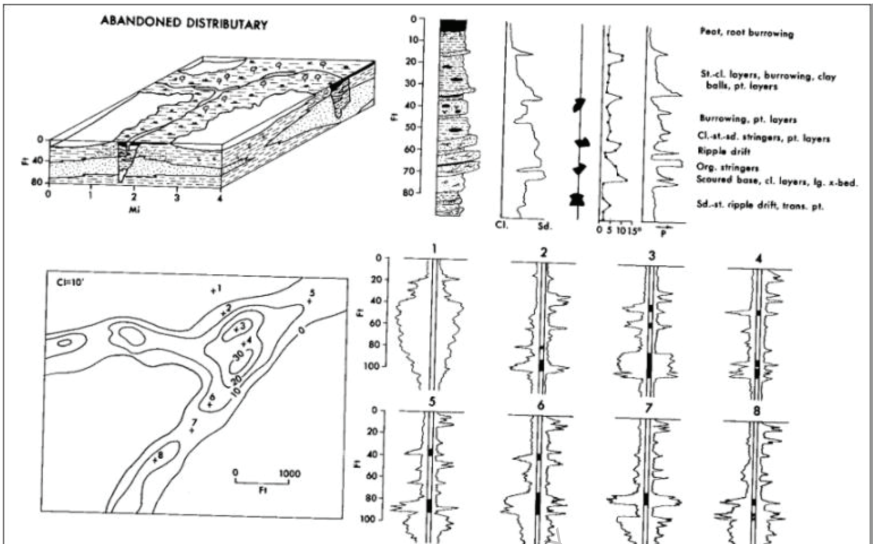

Fig. 13—Summary diagram illustrating the major characteristics of the abandoned distributary deposits in the lower delta plain.

Figure 5

Figure 5 Abandoned Distributary Stylised Example (Source Unknown)

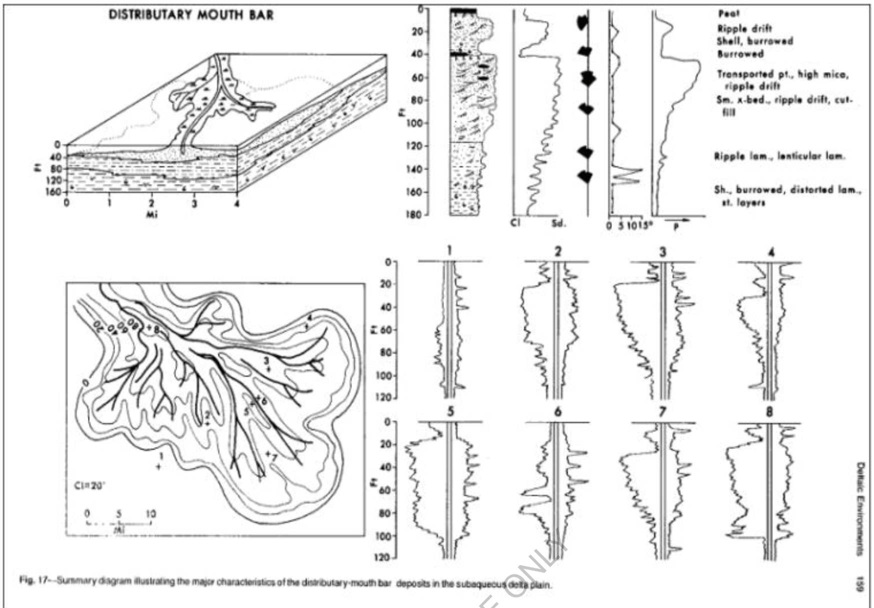

Fig. 17--Summary diagram illustrating the major characteristics of the distributary-mouth bar deposits in the subaqueous delta plain.

Figure 6

Figure 6 Abandoned Distributary Mouth Bar Stylised Example (Source Unknown)

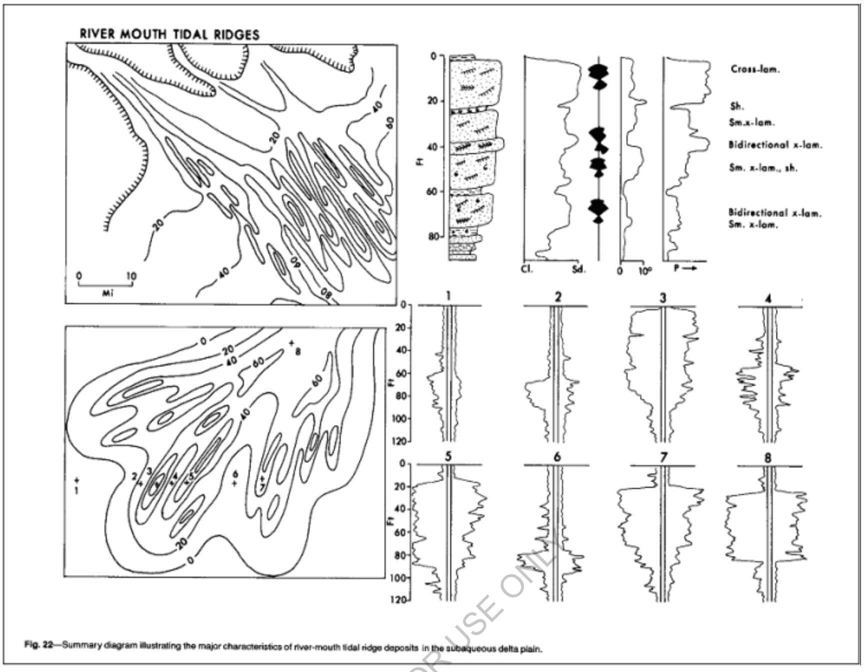

Figure 7

Figure 7 River Mouth Bar Tidal Ridges Stylised Example (Source Unknown)

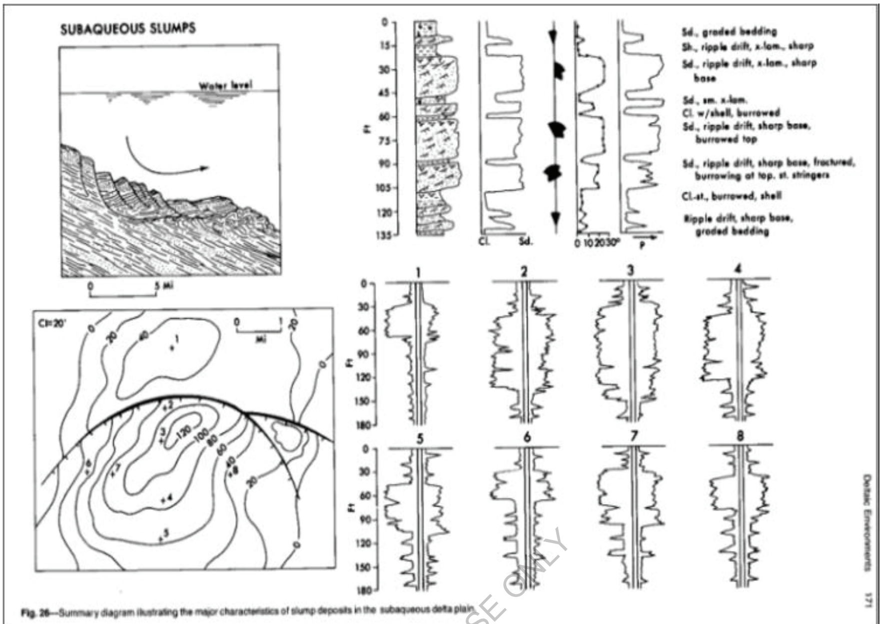

Figure 8

Figure 8 Subaqueous Slumps Stylised Example (Source Unknown)

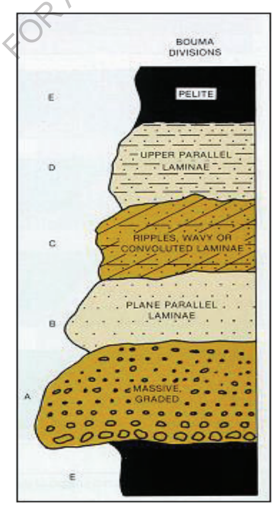

Figure 9

Figure 9 Bouma Units for a Turbidite. From Fundamentals of Dip Log Analysis Atlas Wireline Services Western Atlas (Bigelow, 1987)

Water release structures are a characteristic of turbidites. These can destroy the bedding and other characteristics that are typified by the basic Bouma cycle. A technique, utilizing the dip data from slumps has been devised based on folding. In certain channel turbidites, the slump planes will have a tendency to be perpendicular to the channel direction (Ottesen, C., Personal Communication 1999) which is illustrated in Figure 10.

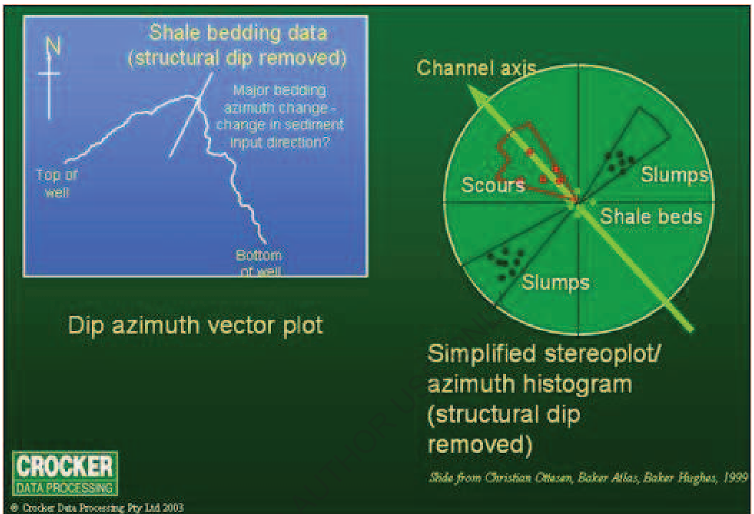

Figure 10

Figure 10 Use of walkout plot and rose plot to identify channel axis and paleocurrent direction.

Shallow Marine

The shallow marine environment is typified by shore face beaches, barrier islands, lagoons, estuaries and other deposits. Tidal flats generally have a bimodal dip distribution illustrative of the tidal variations. In marsh areas and lagoon areas, bioturbation usually destroys the bedding within the interval. Barrier bars and shore face environment will show a generally pro-grading dip trend. Again the presence of bioturbation will impact on the identification of the facies.

An example of a shore face environment image is illustrated below:

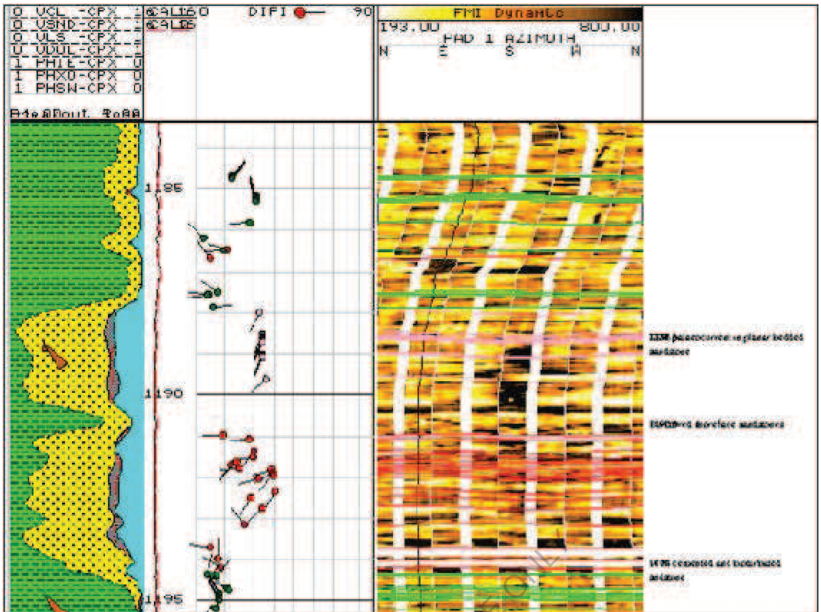

Figure 11

Figure 11 Shore face sand body showing consistent SW pro-gradation.

When bioturbation occurs the images will look like the following:

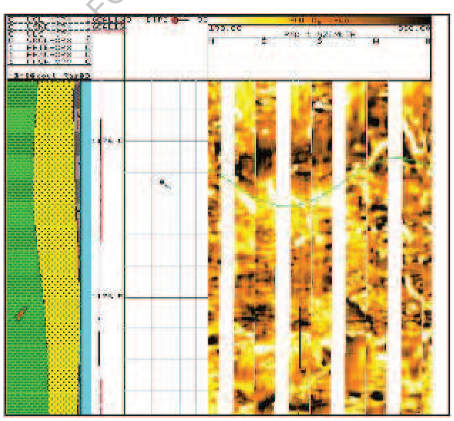

Figure 12

Figure 12 Shore face sand body with bioturbation.

By combining the bioturbation index discussed in Sedimentologic Dip Interpretation Techniques with the dip picking and images, a reasonable picture of bioturbated zones and their spatial arrangement can be illustrated. This information can be helpful in showing zones of high and low permeability.

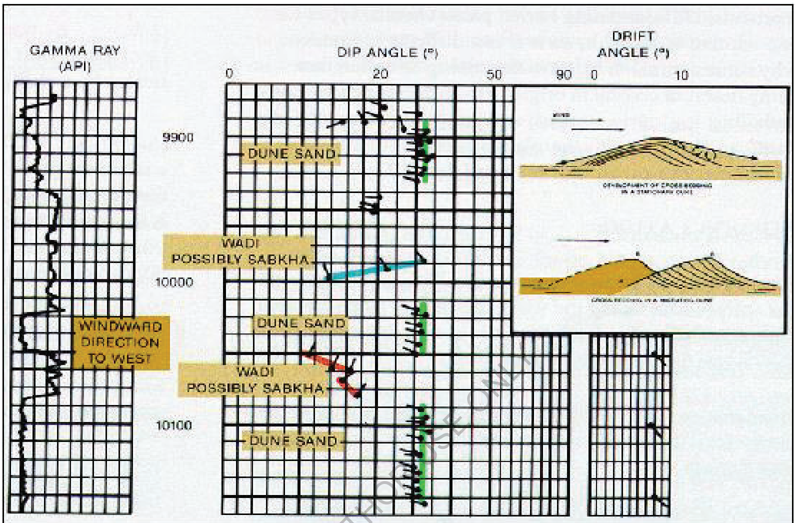

Figure 13

Figure 13 Dune sand "Fundamentals of Dip Log Analysis Atlas Wireline Services Western Atlas (Bigelow, 1987)"

magelog Interpretation: Carbonate Environments

Carbonates are sediments that are formed through biologic processes. Typically when referring to carbonates, corals and stomatolites immediately come to mind, however there are also oolitic shoals and chalks which increase the diversity in interpreting images acquired in these environments.

Dipmeter data acquired in carbonate environments was observed early on to reflect drape patterns over reefs. This structural trend caused by differential compaction permitted the use of the dipmeter data (and today image data) to identify the direction to the centre of the reef. As the drape increases with dip magnitude and is oriented away from the reef centre, the direction of the reef was usually 180 degrees from this down dip trend. Such a trend is illustrated below:

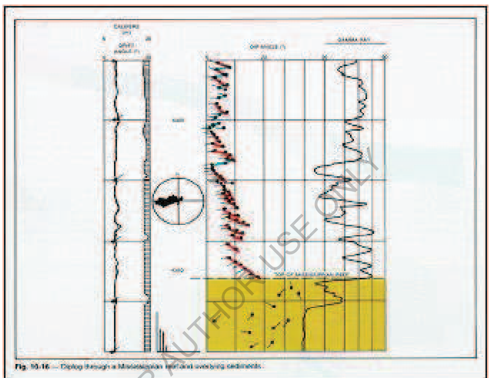

Figure 1

Figure 1 Drape over carbonate reef. Ref: Fundamentals of Dip Log Analysis Atlas Wireline Services Western Atlas (Bigelow, 1987).

Inside the reef, the fabrics associated with the various environments of deposition will be varied. Unlike clastic sediments, there is no notion of depositional direction and the reservoir quality is a function of position within the reef. The following figure illustrates a variety of different facies within a limestone unit:

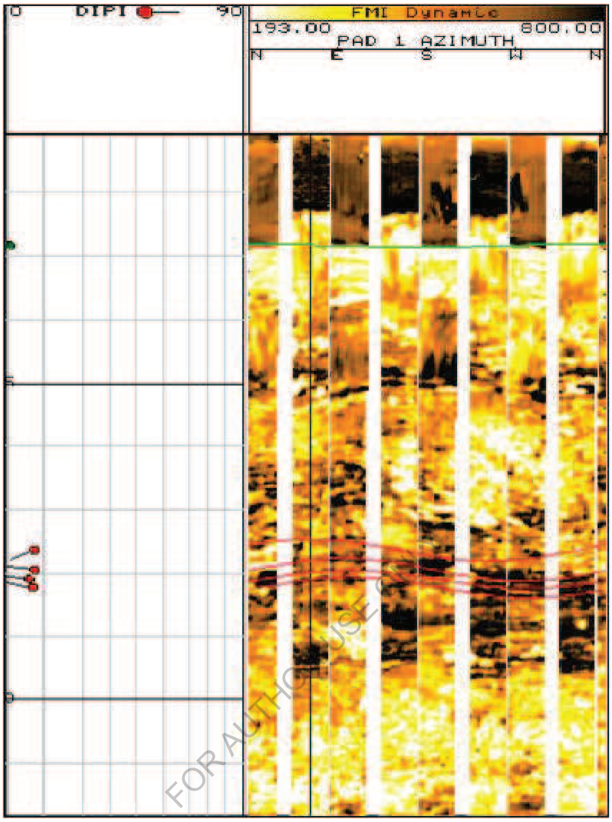

Figure 2

Figure 2 Image over a limestone

In the above example, bedding, bioturbation, fossil fragmentation and potential secondary porosity could be interpreted. In interpreting images like the one above, poses an interesting question of: "Do I classify every feature?" the best approach is to classify dips when available. Identifying and classifying vugs is probably as easy as classifying dips. Finally, a scheme to classify the various other features within the carbonate interval has to be developed to meet the particular interval in question. Best approach is as follows:

1. Identify bedding and classify using an abbreviated clastic scheme consisting of beds, heterolithics, bed boundary and intra/coset boundaries.
2. Classify fractures as conductive and resistive
3. Identify vugs
4. Utilize a combination of visual observations and the fabric index to assign facies.

Facies can be assigned as per Dunham's classification or if definitive information is provided regarding grain type, then Folk's classification can be used as per the following Figure.

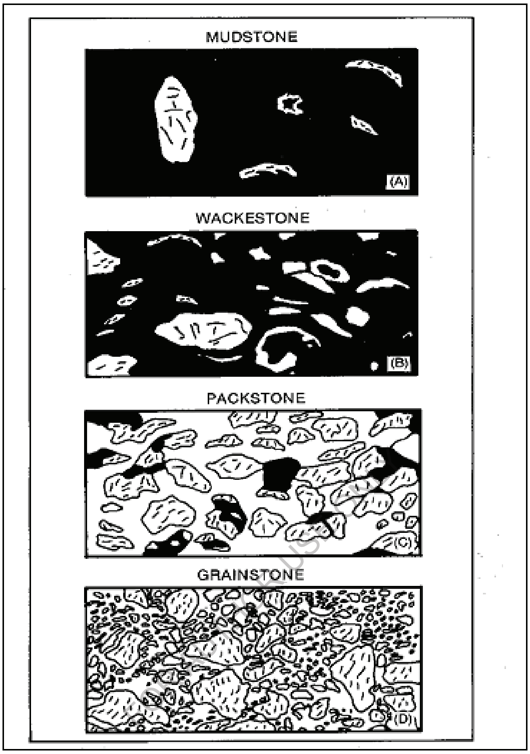

Figure 3

Figure 3 Dunham's Classification Scheme

The overall aim is to obtain a realistic idea of location on reef and spatially where better or more prospective reservoir may exist as well as typical parameters for the reef type as illustrated below:

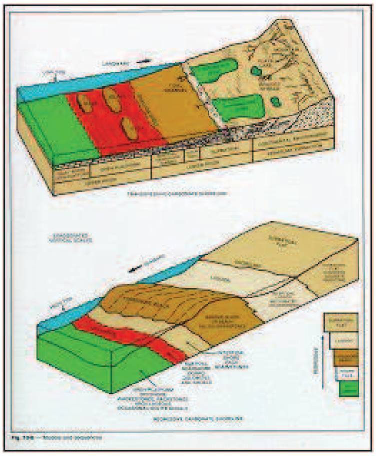

Figure 4

Figure 4 Typical Reef. Ref: Fundamentals of Dip Log Analysis Atlas Wireline Services Western Atlas (Bigelow, 1987).

Imagelog Interpretation: Thin Bed Analysis

Standard OH logs measurement do not respond accurately to the formation in the presence of thin beds (< 1 Ft)

This is mostly de to the vertical resolution of the OH tools and also to their physical limitations.

The SP log respond very poorly in thin bed and the correction charts often do not correct the log properly since we cannot measure the bed thickness accurately enough.

GR counts from adjacent shales in thin sand beds results in very high readings of the GR over such thin sand sections. The Density and Neutron logs are all responding poorly in thin beds and quantitative measurements are unreliable in thin beds..

The Deep induction tool has a vertical resolution of 5 feet but is measuring the horizontal conductivity of the formation. The induction currents will flow through the most conductive paths (shales) and will not see high resistivity sands clearly. New tri-axial induction tools can partially correct for thin bed effects in isotropic formations.

A 200 foot high thin bed sand shale sequence (50/50) can have 100 foot of clean hydrocarbon bearing sands that are completely missed by standard OH logs.

Large gas shows over thick shale can be the results of thin sands within the shale that is invisible to standard OH logs.

Formation micro scanners on the other hand have a vertical resolution of 0.2 inch or better and can identify thin beds and in certain conditions can be used to make quantitative log interpretation including porosity, permeability, volume of shales and water saturations.

CONDITIONS to obtain valid results from Imagelog thin bed processing.

- Good hole conditions with the hole on gauge and with reliable readings from the micro scanner tool.
- The availability of core data (Porosity and permeability) over sections of the thin sands to validate the results.
- Water saturation measurements are based on the assumption that SWirrr and the sand porosity remains relatively constant over the sand-shale sequence.

Imagelog Interpretation: Reservoir Heterogeneity

The changes in carbonate rock fabric are captured in image logs as variation in conductive and resistive image texture proportion. This in turn is captured by variation in the FMI porosity distribution histogram in the form of changes in amplitude, width and skewness of the porosity map. A special technique was adapted to capture the above changes in porosity histograms and converted into a single heterogeneity index curve. This curve can be utilized to predict petrophysical facies changes in the reservoir, stacking patterns and high light degree of reservoir property variability and uncertainties in the conventional coarse core plug measurements. As a result the FMI petrophysical properties is used to identify small scale changes in the rocks fabric and can be used to enhance and compute Vclay, Vmatrix and water saturations within the formation.

Reservoir Quality Analysis

The heterogeneity analysis is computed by integrating PHIT from OH Log analysis and high resolution azimuthal FMI logs in order to capture fine scale porosity variability across the wellbore. The permeability index is calculated using a derivation of the Timur porosity to permeability transform that takes into account the secondary porosity. The following inputs are used in the Timur perm equation:

- Total porosity including vclay/silt fraction
- Primary porosity (average peak porosity from histogram)
- Porosity in the high porosity tail 0.15 porosity units above primary porosity
- Standard Timur coefficient
- Coefficient that impacts the variation that affects impact the secondary to primary porosity ratio has on the permeability.

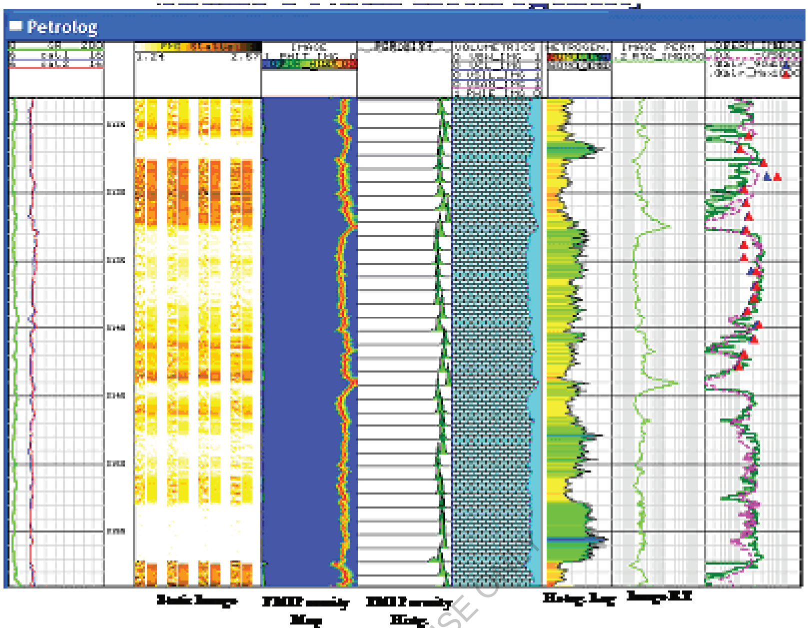

Figure 1

Figure 1: Summary of quantitative heterogeneity analysis

Figure 1 shows a summary of quantitative heterogeneity analysis to estimate secondary and matrix porosity changes near borehole. Amount of secondary porosity is shown in Track 4 (green curve) and average h.

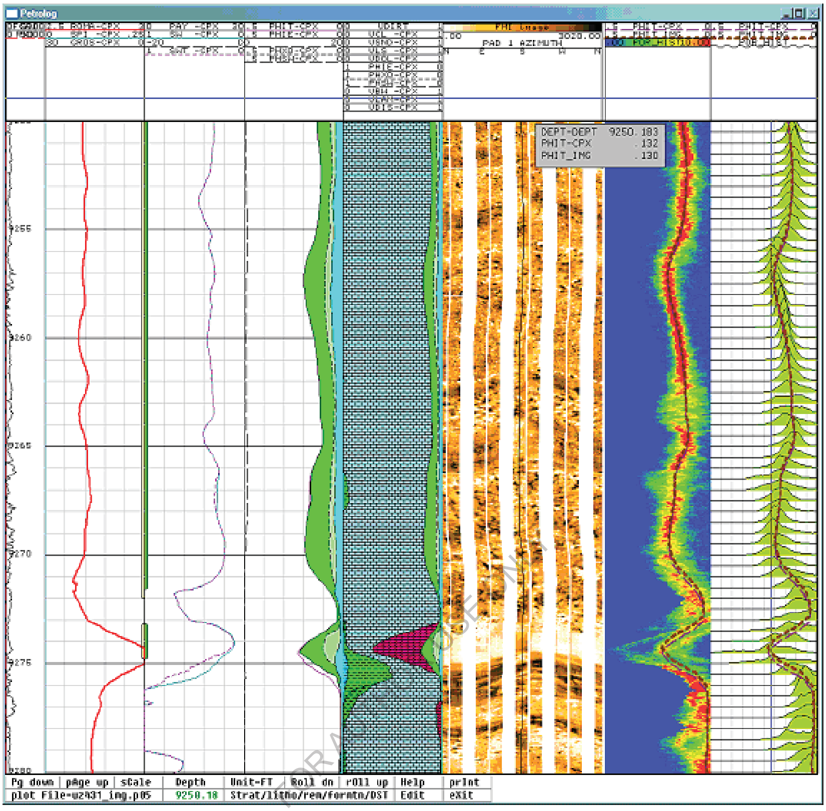

Figure 2: FMI Heterogeneity Analysis

Figure 2 shows the FMI porosity in a black curves. Track 5 shows the porosity histogram distribution. Track 7 shows porosity heterogeneity (heterogeneity increasing to the left). RT computed from FMI is in Track 8. FMI permeability (green curve) and core plug permeability are shown in Track 9.

Neural Network Facies and Flow Units Prediction

Both Supervised and un-supervised neural network techniques were used in core facies and flow units (electrical facies) predictions. The neural network approach used is Back Propagation Neural Network or BPNN for short. It is the most widely used neural network system and most well known supervised learning techniques. It trains via a training set containing a number of input and output pairs of data. It learns from an underlying generalized function of the data instead of memorizing the training data.

This is particularly important where some FMI data are noisy due to tool sticking and borehole conditions. It uses Self-Organising Map (SOM) algorithms and Learning Vector Quantization (LVQ) algorithms to classify the training input logs into a number of classes (or sub classes). After classification process, each class will contain input logs of similar characteristic. Each of these classes will be individually trained by using BPNN. Figure 3 represents a general workflow implemented in predicting facies and flow units.

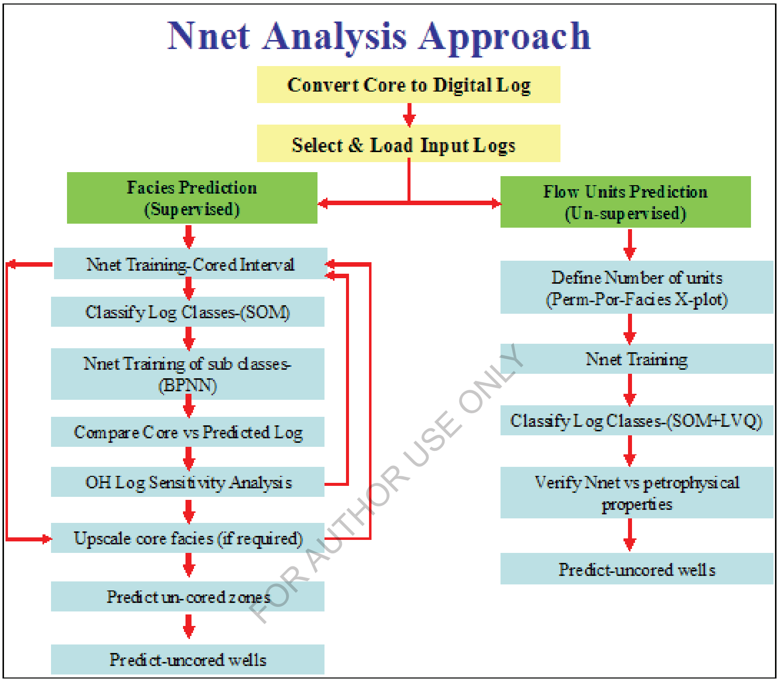

Figure 3: Neural Network Facies Determination Workflow

The core facies, lithologies and grain-size provided by core lab are converted to a digital log by assigning a consistent number code for each representative description (see Figure 4)

Depth From	Depth To	Core No	Lithology	LithTCode	Grain size	GrainTCode	Facies Code	Facies Tcode
2452.84	2453.27	1	Lime mudstone	1	Upper silt	1	LM	1
2453.27	2453.31	1	Lime mudstone	1	Upper silt	1	LM	1
2452.3	2452.45	1	Clotted wackestone	3	Lower veryfine	2	LWsg	2
2453.55	2454.08	1	Clotted wackestone	3	Lower veryfine	2	LWsg	2
2454.55	2455.1	1	Clotted wackestone	3	Lower veryfine	2	LWsg	2
2455.1	2455.31	1	Clotted wackestone	3	Lower veryfine	2	LWsg	2
2452.45	2452.84	1	Clotted wackestone	3	Upper veryfine	3	LWsg	2
2453.31	2453.55	1	Skeletal wackestone	4	Upper veryfine	3	LWsg	2
2454.08	2454.39	1	Skeletal wackestone	4	Upper veryfine	3	LWsg	2
2455.31	2455.58	1	Skeletal wackestone	4	Upper veryfine	3	LWsg	2
2454.39	2454.55	1	Floatstone/wackestone	5	Upper fine	5	LWsg	2
2482.38	2483.29	2	Floatstone/packstone	7	Lower medium	6	LTPs	3
2483.29	2483.49	2	Floatstone/packstone	7	Lower medium	6	LTPs	3
2483.79	2483.87	2	Floatstone/packstone	7	Lower medium	6	LTPs	3
2483.87	2484.44	2	Floatstone/packstone	7	Lower medium	6	LTPs	3
2492.83	2493.01	3	Muddy rudstone	2	Lower verycoarse	10	LRm(mu)	4
2488.08	2488.4	2	Muddy rudstone	2	Upper verycoarse	11	LRm(mu)	4
2488.01	2488.12	3	Muddy rudstone	2	Upper verycoarse	11	LRm(mu)	4
2488.12	2488.45	3	Muddy rudstone	2	Upper verycoarse	11	LRm(mu)	4
2493.01	2493.37	3	Muddy rudstone	2	Upper verycoarse	11	LRm(mu)	4
2505.55	2505.88	3	Muddy rudstone	2	Upper verycoarse	11	LRm(mu)	4
2508.88	2509.15	4	Muddy rudstone	2	Upper verycoarse	11	LRm(mu)	4
2529.85	2530.75	5	Muddy rudstone	2	Upper verycoarse	11	LRm(mu)	4
2497.5	2497.85	3	Muddy rudstone	2	Lower granular	12	LRm(mu)	4
2498.15	2498.41	3	Muddy rudstone	2	Lower granular	12	LRm(mu)	4
2502.31	2502.75	3	Muddy rudstone	2	Lower granular	12	LRm(mu)	4
2504.78	2505.01	3	Muddy rudstone	2	Lower granular	12	LRm(mu)	4
2512.51	2512.78	4	Muddy rudstone	2	Lower granular	12	LRm(mu)	4
2531.43	2531.59	5	Muddy rudstone	2	Lower granular	12	LRm(mu)	4
2493.37	2494.5	3	Muddy rudstone	2	Upper granular	13	LRm(mu)	4
2502.9	2503.51	3	Muddy rudstone	2	Upper granular	13	LRm(mu)	4
2534.8	2535.48	5	Muddy rudstone	2	Upper granular	13	LRm(mu)	4
2535.48	2536.01	5	Muddy rudstone	2	Upper granular	13	LRm(mu)	4
2539.41	2540.08	5	Muddy rudstone	2	Upper granular	13	LRm(mu)	4
2540.55	2540.95	5	Muddy rudstone	2	Upper granular	13	LRm(mu)	4
2471.18	2471.22	2	Floatstone/grainstone	9	Upper medium	7	LRm	5
2471.22	2471.41	2	Floatstone/grainstone	9	Lower coarse	8	LRm	5
2455.87	2456.1	1	Rudstone	10	Lower granular	12	LRm	5
2456.1	2456.63	1	Rudstone	10	Lower granular	12	LRm	5
2456.78	2456.89	1	Rudstone	10	Lower granular	12	LRm	5
2470.95	2471.18	2	Rudstone	10	Lower granular	12	LRm	5
2471.41	2471.51	2	Rudstone	10	Lower granular	12	LRm	5
2474.18	2474.84	2	Rudstone	10	Lower granular	12	LRm	5
2475.69	2475.83	2	Rudstone	10	Lower granular	12	LRm	5
2475.83	2475.94	2	Rudstone	10	Lower granular	12	LRm	5
2477.83	2477.97	2	Rudstone	10	Lower granular	12	LRm	5

Figure 4: Tabular Results of Neural Network Facies Analysis

The Facies Identification process is done via the following general process:

1) Convert core facies into digital log

2) Identification and grouping of Facies described by the Core Analysis

3) Use these to train the system to produce facies using individual wells to create training set to predict each other well. This will reinforce stability of some flow unit groups and the lack of stability of others. Well-1 training set is used to predict Well-2 core facies.

4) Predict the core facies for each well using the training set to identify where prediction matches and diverges from lithofacies as identified from core.

5) Upscale the model by doing two things: A) reduce (adjust) image derived curve resolution or openhole logs resolution. B) Diminish number of lithofacies/core facies to a prescribed number.

6) Repeat steps 1-4

The flow units prediction was done by using an unsupervised self organizing map (SOM) which uses the same technology as used for facies but without any assumed flow unit property to lithofacies relationship. By using the core lithology as outlined above, the assumption is made that the properties to be determined are specifically associated with lithologic/core facies. Petrophysical properties tend to be a cluster with a minimum and maximum and are more directly related to pore throat diameter and other parameters that directly affect flow. These may (or may not) be related to lithology.

The flow units identification process was done via the following general process:

1) Take the conventional openhole logs at best sample rate (6 inches usually) and the curves generated from the porosity histogram relevant to porosity, permeability and heterogeneity for each well.

2) Use these to train the system to produce flow unit groups. The number of groups is arbitrarily set as the same number of core-facies.

3) Predict the heterogeneity curve for each well using the training set to identify where prediction matches and diverges from heterogeneity curve.

4) Repeat procedure using individual wells to create training set to predict each other well. This will reinforce stability of some flow unit groups and the lack of stability of others.

5) Upscale the model by doing two things: A) reduce image derived curve resolution to 6 inches or openhole resolution. B) Diminish number of flow unit groupings to a prescribed number.

6) Repeat steps 1-4

The FMI data is at 0.2 inch and produces extremely high resolution porosity and permeability variations. The heterogeneity curve is a curve that identifies at a specific depth increment the variation in the porosity distribution within the rock, which represents a critical flow unit property. By using this curve as the prediction curve, a set of groupings can be generated that are independent of the core lithology/facies.

Imagelog Interpretation: Borehole Mechanics

Images by virtue of the fact that they have 4 or more calipers, permit the borehole orientation and any ovality to be determined. By knowing this ovality, the horizontal stress field can be oriented and used in further analysis such as:

- Sanding analysis
- Borehole breakout analysis
- Borehole stability

The example below shows how one can orient the stress field:

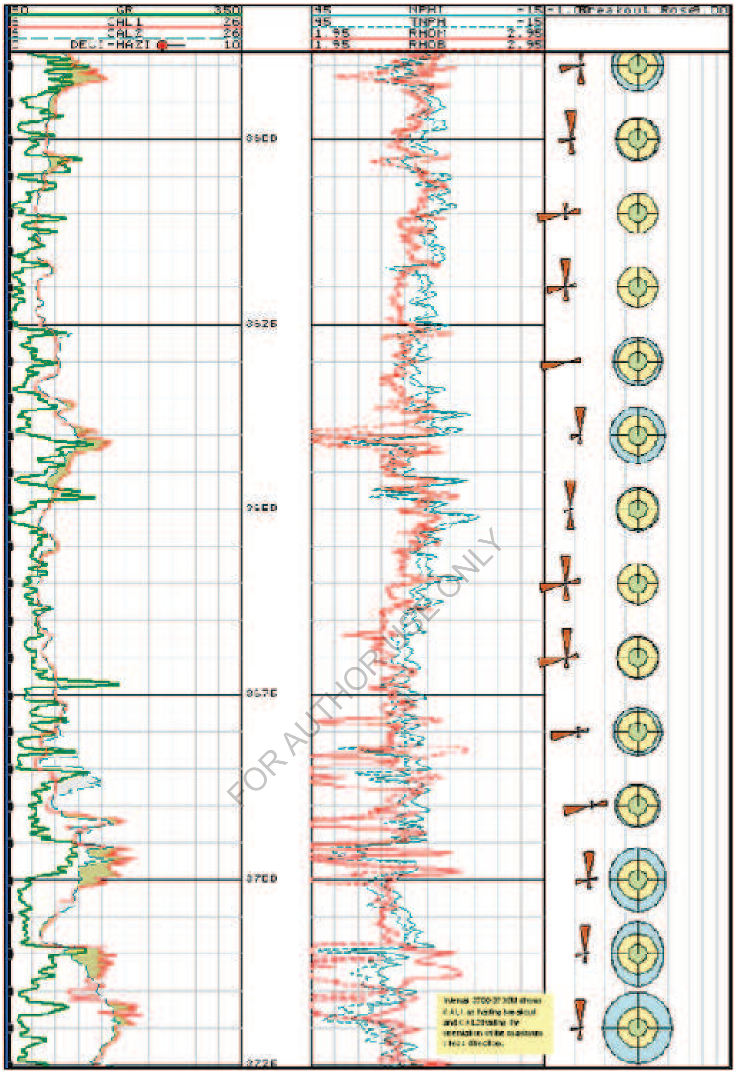

Figure 1 Borehole ovality from calipers.

Further information about the stress field can be identified from other features seen on the images. Tensile fractures will occur in the orientation of the maximum stress direction. These result from over balanced mud causing the rock to fail. An example of borehole induced tensile fractures is illustrated below:

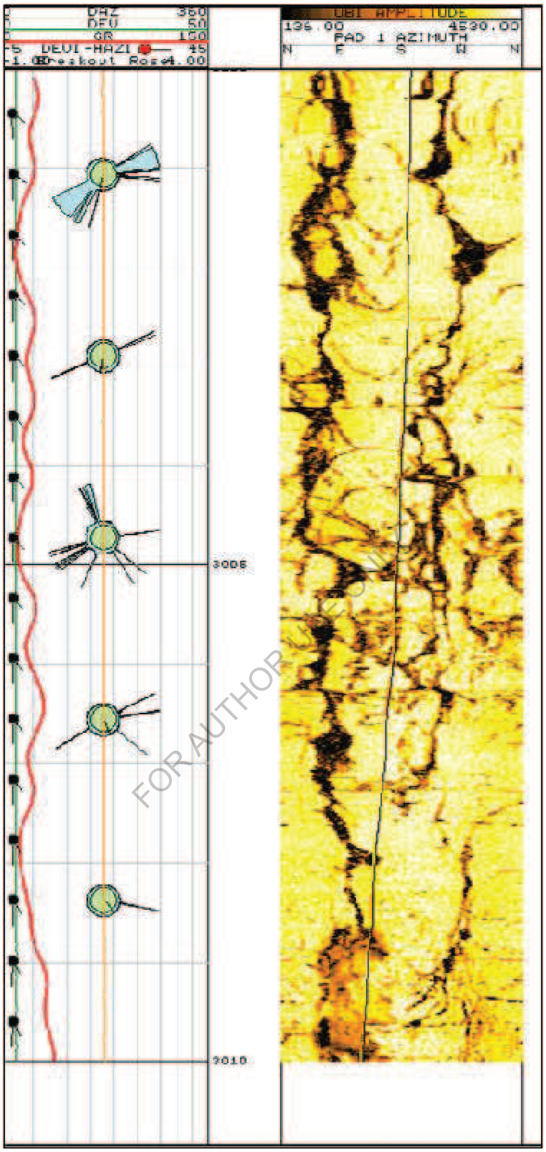

Figure 2 Tensile Fractures.

Tensile fractures or Breakouts are produced when very different conditions are met. In the case of tensile fractures, the force exerted by the mud weight has to be greater than the forces exerted in a horizontal direction in the borehole. This is illustrated by the following figure:

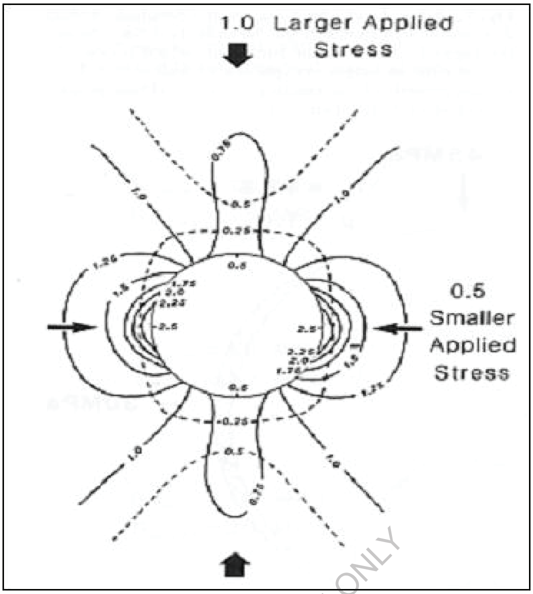

Figure 3 Stress Regime around a borehole where a bi-axial stress regime is applied and ratio is 2:1(Reproduced from Figure 5, Bell , 1990).

Breakouts occur when the tangential stresses exceed the shear stress of the rock (p 309, Bell, 1990) Shear fractures form in the lunate regions (represented by the smaller shear stress areas in Figure 191) and breakouts occur. Also, in Figure 191, the stress amplification causes a negative stress envelope in the maximum horizontal stress direction. This coincides with the maximum stress orientation. Extensional Tangential stress is caused in this region and causes the rock to part when a pressure such as overbalanced mud weight is applied or hydraulic fracturing is undertaken. In a vertical well the orientation of hydraulically induced fractures will be in the direction of the maximum horizontal stress direction

Ref: Bell, J. S., Investigating stress regimes in sedimentary basins using information from oil industry Wireline logs and drilling records. From Hurts A, Lovell, M. A. & Morton A. C. (eds), 1990, Geological Applications od Wireline Logs Geological Society Special Publication No. 48, pp 305-325

Stereonets

Displaying Stereonets

Any tadpole presentation can be accompanied by Stereonets that are plotted automatically anywhere on the plot with multiple presentations.

Stereographic projections can also be generates as individual plots in the workflow explorer window using Graphics + Stereographic Projections. See Stereographic Projections

Step By Step Procedures

Step 1: Plot the formation image with at least one set of dip results in one track. See Figure 1.

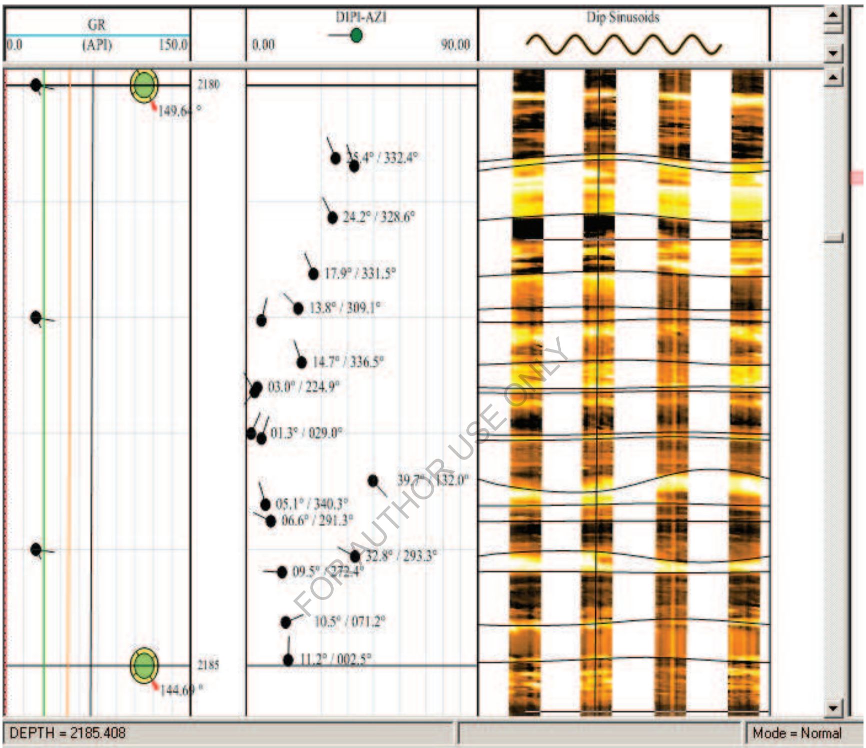

Figure 1 show an FMS plot with the dip plotted in track 3

Step 2: Click on the icon IMAGELOG MAIN Menu. to obtain figure 2 then select Stereonet to obtain figure 3.